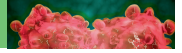


## RESEARCH ARTICLE

## ENVIRONMENTAL MICROBIOLOGY



# Distinct bacterial succession and functional response to alginate in the South, Equatorial, and North Pacific Ocean

John Paul Balmonte<sup>1,2</sup> | Helge-Ansgar Giebel<sup>3</sup> | Carol Arnosti<sup>1</sup> |  
 Meinhard Simon<sup>3</sup> | Matthias Wietz<sup>3,4</sup>

<sup>1</sup>Department of Earth, Marine and Environmental Sciences, The University of North Carolina at Chapel Hill, Chapel Hill, NC, USA

<sup>2</sup>Department of Earth and Environmental Sciences, Lehigh University, Bethlehem, PA, USA

<sup>3</sup>Institute for Chemistry and Biology of the Marine Environment, University of Oldenburg, Oldenburg, Germany

<sup>4</sup>Deep-Sea Ecology and Technology, Alfred Wegener Institute Helmholtz Centre for Polar and Marine Research, Bremerhaven, Germany

## Correspondence

John Paul Balmonte, Department of Earth and Environmental Sciences, Lehigh University, Bethlehem, PA, USA.  
 Email: [jpb422@lehigh.edu](mailto:jpb422@lehigh.edu)

Matthias Wietz, Deep-Sea Ecology and Technology, Alfred Wegener Institute Helmholtz Centre for Polar and Marine Research, Bremerhaven, Germany.  
 Email: [matthias.wietz@awi.de](mailto:matthias.wietz@awi.de)

## Present addresses

John Paul Balmonte, Department of Earth and Environmental Sciences, Lehigh University, Bethlehem, Pennsylvania, USA; and Matthias Wietz, Deep-Sea Ecology and Technology, Alfred Wegener Institute Helmholtz Centre for Polar and Marine Research, Bremerhaven, Germany.

## Funding information

UNC Global Partnership Award; Bundesministerium für Bildung und Forschung, Grant/Award Number: 03G0248A; Division of Ocean Sciences, Grant/Award Numbers: OCE-1332881, OCE-1736772; Deutsche Forschungsgemeinschaft, Grant/Award Numbers: TRR51, WI3888/1-2

## Abstract

The availability of alginate, an abundant macroalgal polysaccharide, induces compositional and functional responses among marine microbes, but these dynamics have not been characterized across the Pacific Ocean. We investigated alginate-induced compositional and functional shifts (e.g., heterotrophic production, glucose turnover, hydrolytic enzyme activities) of microbial communities in the South Subtropical, Equatorial, and Polar Frontal North Pacific in mesocosms. We observed that shifts in response to alginate were site-specific. In the South Subtropical Pacific, prokaryotic cell counts, glucose turnover, and peptidase activities changed the most with alginate addition, along with the enrichment of the widest range of particle-associated taxa (161 amplicon sequence variants; ASVs) belonging to *Alteromonadaceae*, *Rhodobacteraceae*, *Phormidiaceae*, and *Pseudoalteromonadaceae*. Some of these taxa were detected at other sites but only enriched in the South Pacific. In the Equatorial Pacific, glucose turnover and heterotrophic prokaryotic production increased most rapidly; a single *Alteromonas* taxon dominated (60% of the community) but remained low (<2%) elsewhere. In the North Pacific, the particle-associated community response to alginate was gradual, with a more limited range of alginate-enriched taxa (82 ASVs). Thus, alginate-related ecological and biogeochemical shifts depend on a combination of factors that include the ability to utilize alginate, environmental conditions, and microbial interactions.

## INTRODUCTION

Polysaccharides constitute a substantial fraction of dissolved and particulate marine organic matter, fuelling microbial heterotrophy in the oceans (Amon & Benner, 1996; Arnosti et al., 2021). As a high molecular weight source of carbon, polysaccharides are typically hydrolysed to oligomers or their constituent monomers, either extracellularly or within the periplasm (Arnosti, 2011;

Reintjes et al., 2017). Hydrolysis of polysaccharides requires the production of degradative enzymes which, depending on the type of polysaccharide and its structural complexity, are diverse and numerous (Sichert et al., 2020). Such an energetically costly investment requires that microorganisms regulate enzymatic production based on substrate presence and metabolic needs (Koch et al., 2019; Traving et al., 2015). Microbial taxa that specialize in polysaccharide utilization may remain minimally

This is an open access article under the terms of the [Creative Commons Attribution-NonCommercial](https://creativecommons.org/licenses/by-nc/4.0/) License, which permits use, distribution and reproduction in any medium, provided the original work is properly cited and is not used for commercial purposes.

© 2024 The Authors. *Environmental Microbiology* published by Applied Microbiology International and John Wiley & Sons Ltd.



active until substrates become available, inducing compositional and metabolic shifts (Teeling et al., 2012). Thus, changes in polysaccharide availability can distinctly influence microbial community dynamics, both in composition and function.

Alginate, a polysaccharide comprised of the uronic acids mannuronate and guluronate (Rehm, 2009) and with gelling properties in seawater (Abka-Khajouei et al., 2022), is produced by macroalgae at up to 60% of dry weight (Draget et al., 2005). Alginate is contained in coastal (e.g., *Fucus* and *Saccharina*) and open ocean taxa such as *Sargassum* (Davis et al., 2021; Rosado-Espinosa et al., 2020; Yip et al., 2020), representing a nutrient source for both coastal and open ocean microbes. Several studies have shown that alginate can stimulate distinct compositional shifts among microbial communities in temperate (Bunse et al., 2021; Enke et al., 2019; Mitulla et al., 2016; Thomas et al., 2021) and polar waters (Jain et al., 2020; Wietz et al., 2015). Site-specific patterns in bacterial succession indicated differing alginolytic potentials in the Southern and Atlantic Oceans (Wietz et al., 2015). In a Svalbard fjord, *Colwellia*, *Polaribacter*, and *Pseudoalteromonas* peaked following alginate availability (Jain et al., 2020). Furthermore, alginate induced distinct responses among particle-associated (PA) versus free-living (FL) bacteria from a macroalgae-rich habitat; however, that study used a mix of synthetic polysaccharide particles instead of pure alginate (Bunse et al., 2021). PA taxa expressed a wide range of alginate lyases, whereas the strong response of one FL taxon likely corresponded to its ability to utilize oligomers from alginate degradation (Bunse et al., 2021).

Alginate degradation and utilization involves many genes that are mostly found within classes *Bacteroidia* and *Gammaproteobacteria* (Cheng et al., 2020; Koch et al., 2019; Neumann et al., 2015; Thomas et al., 2012; Thomas et al., 2021). Their repertoires of alginate lyase genes, many of which are encoded in polysaccharide utilization loci (PULs), likely underpin rapid responses upon alginate availability (Bunse et al., 2021; Thomas et al., 2021). Metabolic byproducts from alginate degradation may also promote the growth of taxa without alginolytic capacities due to cross-feeding (Enke et al., 2019; Thomas et al., 2021; Wietz et al., 2015). These processes can coincide with a suite of physiological and functional changes, including increased cell abundance and protein production (Jain et al., 2020; Mitulla et al., 2016; Thomas et al., 2021). However, the extent to which alginate modulates microbial community succession and enzymatic activities in distinct biogeographic provinces (e.g., oligotrophic gyres, upwelling areas, frontal zones) within a single ocean is less understood. This knowledge gap is especially apparent in the open waters of the Pacific Ocean.

In this study, we used experimental mesocosms to investigate alginate-induced responses of bacterial communities in three biogeographic provinces of the Pacific Ocean: the South Pacific Subtropical Gyre (SPSG, herein South Pacific), the Pacific North Equatorial Current (PNEC, herein Equatorial Pacific) and the North Pacific Polar Frontal region (NPPF, herein North Pacific). We identified differences in PA versus FL community succession by amplicon sequencing of 16S rRNA genes. To quantify alginate-induced physiological and functional shifts, we measured prokaryotic cell abundances, heterotrophic prokaryotic production, glucose turnover, and enzymatic activities using a range of peptide, glucose, and polysaccharide substrates. We asked the following questions: (1) Does the speed and magnitude of community succession in response to alginate vary across prokaryotic communities and biogeographic provinces, and to what extent do PA versus FL communities differ in their compositional response? (2) Does alginate select for a similar or distinct subset of the community across different biogeographic provinces? (3) Do community shifts coincide with functional alterations, and are these changes consistent with the timing and intensity of community responses? Our study provides insight into the ecological and biogeochemical implications of polysaccharide availability in open oceanic waters across biogeochemical provinces and a wide latitudinal range.

## EXPERIMENTAL PROCEDURES

### Sample collection, physicochemical parameters, and experimental setup

Mesocosm experiments were conducted in the South (Longhurst province SPSG; 26.99° S, 178.21° W), Equatorial (province PNEC; 4.66° S, 179.40° W), and North Pacific (province NPPF; 45.00° N 178.75° W) during cruise SO248 aboard RV *Sonne* (Giebel et al., 2021; Milke et al. 2022). Water was sampled from a depth of 20 m in the South and North Pacific, and at 75 m in the Equatorial Pacific to sample the core of the equatorial upwelling (as determined by a preceding CTD cast). Physicochemical parameters, including concentrations of Chlorophyll *a* (chl *a*), particulate organic carbon (POC), and particulate organic nitrogen (PON) were measured according to protocols described elsewhere (Giebel et al., 2021).

At each location, seawater was collected and distributed in six 20 L acid-washed Nalgene bottles for triplicate alginate incubations, and triplicate unamended controls. Seawater was not pre-filtered; thus, it contained the entire ambient microbiome, including bacteria, archaea, phytoplankton, and larger protists. Hence, observed responses might include non-bacterial dynamics. Per the alginate incubation bottle, 22.5 mL



of 1% w/v sterile-filtered alginate (Sigma A2158) was added, corresponding to about 0.02 g alginate L<sup>-1</sup>. Bottles were incubated close to in situ temperature under a 12:12 h light–dark cycle. Changing light regimes potentially resulted in varying phytoplankton activities, with corresponding effects on the exudation of other organic matter that potentially fuelled microbial heterotrophy. In turn, grazing and other types of interactions were presumably affected as well; thus, the observed responses may also be related to other factors. After 1, 3, and 6 days of incubation (d1, d3, d6), 3 L were drawn from individual bottles and processed for various analyses as described below.

### Prokaryotic cell counts, heterotrophic prokaryotic production, and glucose turnover

Detailed methods for these measurements can be found in a separate study (Giebel et al., 2021). Briefly, microbial cells (<50 µm) were stained using SYBR Green and measured using a BD Accuri C6 flow cytometer (BD Biosciences, NJ). Heterotrophic prokaryotic production (HPP) was measured either on 10 or 20 mL of sample using <sup>14</sup>C-leucine (12.1 GBq mmol<sup>-1</sup>, Hartmann Analytic, Germany) incubated for 4–8 h following Simon et al. (2004). <sup>14</sup>C-leucine incorporation rates were converted to HPP using a conversion factor of 3.05 kg C (mol leucine)<sup>-1</sup> according to Simon and Azam (1989). Glucose turnover constants were determined on 10 mL samples through the incorporation of <sup>3</sup>H-glucose (2.22 TBq mmol<sup>-1</sup>, Hartmann Analytic) in samples incubated for 4–8 h, following the protocol by Simon and Rosenstock (2007). All samples were incubated in the dark and as close to in situ temperatures as possible. Data are available in Table S1.

### DNA extraction

Per regime, replicate and sampling point, 500 mL seawater was filtered using a peristaltic pump onto polycarbonate filters (diameter 47 mm; Whatman, UK). Alginate samples were prefiltered through 5 µm to capture the PA fraction, and the flow-through was captured on 0.2-µm filters, representing the FL fraction. Control samples and the ambient seawater (start community) were directly filtered on 0.2 µm filters. All filters were flash-frozen in liquid nitrogen and stored at –80°C. In the home lab, simultaneous extraction of DNA and RNA was done using a modification of Schneider et al. (2017) described in detail under [https://zenodo.org/record/4171148/files/DNA-RNA\\_CoExtraction.pdf](https://zenodo.org/record/4171148/files/DNA-RNA_CoExtraction.pdf). Purified DNA and RNA were sent on dry ice to DNASense (Denmark) for quality control and sequencing.

### Sequencing of 16S rRNA gene amplicons

The V3–V4 hypervariable region of 16S rRNA genes was amplified using primers 341F (CCTACGGGN GGCWGCAG) and 785R (GACTACHVGGGTATC TAATCC) (Klindworth et al., 2013) using both DNA and reverse-transcribed RNA as template, following no. 15044223 Rev. B of the 16S Sequencing Library Preparation protocol (Illumina, San Diego, CA). Amplicons were sequenced with paired-end 2 × 300 bp reads on MiSeq technology and reagent kit v3 (Illumina) following standard guidelines. Detailed information on the sequencing protocol is described in the Supporting Information S1.

### Sequence processing and analysis

Amplicon reads were processed using DADA2 (Callahan et al., 2016) following the standard workflow at <https://benjjneb.github.io/dada2/tutorial.html>, with filtering settings truncLen = c(200, 265), maxN = 0, minQ = 2, maxEE = c(3, 3), and truncQ = 0. Amplicon sequence variants (ASVs) assigned from the ~42,000 quality-filtered, chimera-checked paired reads per sample (Table S2) were taxonomically classified using the Silva v138.1 database (Quast et al., 2013).

### Analysis of differentially abundant ASVs

Differential abundance analysis identified ASVs that were enriched in PA and FL fractions of alginate versus control incubations using the DESeq function in ‘DESeq2’ (Love et al., 2014). The Wald significance test and parametric fitting of dispersions were used to analyse a rarefied dataset containing 10,817 reads per sample, representing 3133 ASVs. Differential abundance analysis was also conducted on an unrarefied dataset but was not possible in the South and Equatorial Pacific due to the prevalence of zeros. Thus, we analysed the rarefied dataset, which provided the additional benefit of avoiding potentially spurious results due to uneven sequencing depths. Separate analyses were conducted for the PA-alginate versus control incubations and for the FL-alginate vs. control incubation. A limitation of these analyses is that the controls are bulk (non-size-fractionated), whereas the alginate samples are size-fractionated to PA (>5 µm) and FL (0.2–5 µm). This experimental decision was due to logistical constraints; the unamended controls were shared with another experiment (beyond the scope of this study) for which the samples were not size-fractionated. We recognize that this approach integrates the alginate response signal with the size-fractionated signal. We increased our likelihood of identifying alginate-specific patterns by aggregating the samples for each size



fraction across all time points (d1, d3, d6) and comparing these to all samples in the control (d1, d3, d6), which maximizes replicates for comparison and statistical power. In addition, we focus downstream analyses and interpretations on highly differentially abundant ASVs ( $\log_2$ -fold change  $\geq 3$  and  $p < 0.01$ ).

## Hydrolytic enzyme activity assays

Enzyme activities were measured in ambient seawater prior to the addition of alginate (d0), as well as pooled water samples from triplicate mesocosms after 6 days. We used two types of hydrolytic enzyme activity assays based on substrate type, either labelled with methylcoumarin (MCA), methylumbelliferyl (MUF) (Hoppe, 1983), or fluoresceinamine (FLA) (Arnosti, 2003). Detailed methods descriptions can be found in a related study (Balmonte et al., 2021); raw data are included here (Table S3). Briefly, five MCA- and two MUF-labelled substrates were used to measure peptidase and glucosidase activities, respectively. To measure peptidases, the following substrates were used: Leucine-MCA (leu) for leucine aminopeptidase, Alanine-Alanine-Phenylalanine-MCA (one-letter amino acid code: AAF) and Alanine-Alanine-Proline-Phenylalanine-MCA (AAPF) for chymotrypsins, as well as Phenylalanine-Serine-Arginine-MCA (FSR) and Butyloxycarbonyl-Glutamine-Alanine-Arginine-MCA (QAR) for trypsin. Glucosidase activities were measured using  $\alpha$ -glucopyranoside ( $\alpha$ -glu) and  $\beta$ -glucopyranoside ( $\beta$ -glu). These assays were carried out with live and killed controls in 96-well plates, and with a final substrate concentration of 100  $\mu$ M. Incubations were stored close to in situ water temperature, and the reported rates—converted from fluorescence values obtained using an Infinite F200 plate reader (Tecan, Switzerland)—are from 12 h incubations.

To measure polysaccharide hydrolase activities, we used FLA-labelled pullulan, laminarin, xylan, fucoidan, arabinogalactan, and chondroitin sulphate (Arnosti, 2003). These substrates are hydrolysed to varying degrees in the Pacific Ocean (Balmonte et al., 2021) and elsewhere (Arnosti et al., 2011; Balmonte et al., 2018; Hoarfrost et al., 2019), and genes encoding these enzymes have been found in diverse bacteria (e.g., Bunse et al., 2021; Neumann et al., 2015; Teeling et al., 2012). Since polysaccharide hydrolysis is measured as a change in molecular weight distribution over time, polysaccharide hydrolase samples (the d0 set, as well as the d6 set) were subsampled upon substrate addition and after 5, 10, 15, and 25 days of incubation. Subsamples were stored at  $-20^\circ\text{C}$  until processing using gel permeation chromatography with fluorescence detection (Arnosti, 2003). Reported rates are the maximum potential rates measured at individual time points (Table S3). Fold change values of hydrolysis rates

were calculated using the following equation:  $(\text{Rate}_{\text{alginate}} - \text{Rate}_{\text{control}}) / \text{Rate}_{\text{control}}$ .

## RESULTS

### Water mass characteristics

Experiments were conducted with seawater from the South, Equatorial, and North Pacific Ocean (Figure 1A). These waters differed in physicochemical characteristics, although the South and Equatorial Pacific were more similar compared with the North Pacific. Water temperature was highest in the Equatorial Pacific ( $28.6^\circ\text{C}$ ) despite being collected at 75 m to sample the deep chlorophyll maximum (Table 1); followed by the South ( $25.2^\circ\text{C}$ ) and the North Pacific ( $5.9^\circ\text{C}$ ). Salinity was highest in the South Pacific (35.6 PSU), and lowest in the North Pacific (33.3 PSU). Phosphate was below the detection limit ( $<0.04 \mu\text{M}$ ) in the South Pacific, and highest in the North Pacific ( $1.3 \mu\text{M}$ ). Concentrations of chl *a* ( $0.8 \mu\text{g L}^{-1}$ ), particulate organic carbon (POC;  $98.7 \mu\text{g L}^{-1}$ ), and particulate organic nitrogen (PON;  $20.5 \mu\text{g L}^{-1}$ ) peaked in the North Pacific, indicating more productive waters. The lowest concentrations of chl *a* ( $0.2 \mu\text{g L}^{-1}$ ), POC ( $34.7 \mu\text{g L}^{-1}$ ), and PON ( $4.1 \mu\text{g L}^{-1}$ ) in the Equatorial Pacific indicated less productive waters.

### Distinct prokaryotic growth and metabolism pre- and post-alginate addition

Prokaryotic cell counts in the ambient water (d0) were lowest and highest in the Equatorial Pacific and North Pacific, respectively ( $4.4 \pm 0.2 \times 10^5 \text{ mL}^{-1}$  and  $7.3 \pm 1.0 \times 10^5 \text{ mL}^{-1}$ ) (Table S1). Initial HPP rates did not scale with cell counts, as the lowest and highest values were observed in the South and Equatorial Pacific, respectively ( $9.6 \pm 1.5 \text{ ng C L}^{-1} \text{ h}^{-1}$  and  $375.2 \pm 30.0 \text{ ng C L}^{-1} \text{ h}^{-1}$ ). Mean glucose turnover at d0 was also decoupled from cell counts and HPP, being lowest and highest in the South ( $0.002 \text{ day}^{-1}$ ) and North Pacific ( $0.088 \text{ day}^{-1}$ ), respectively.

Alginate availability stimulated prokaryotic cell counts, HPP, and glucose turnover at varying rates and to differing maximum levels, which did not scale with starting conditions. While cell counts peaked at d6 for all sites, they reached the highest values ( $13.8 \pm 0.4 \times 10^5 \text{ mL}^{-1}$ ) in the South Pacific (Figure 1B). Alginate-induced changes in HPP varied more, peaking at d1 in the Equatorial Pacific ( $4880 \pm 1817 \text{ ng C L}^{-1} \text{ h}^{-1}$ ), and at d6 in the South and North Pacific. Values at d6 in the South Pacific ( $2971 \pm 385 \text{ ng C L}^{-1} \text{ h}^{-1}$ ) and Equatorial Pacific ( $2711 \pm 224 \text{ ng C L}^{-1} \text{ h}^{-1}$ ) were comparable, and substantially higher than in the North Pacific ( $307 \pm 171 \text{ ng C L}^{-1} \text{ h}^{-1}$ ) (Figure 1B). Glucose turnover was

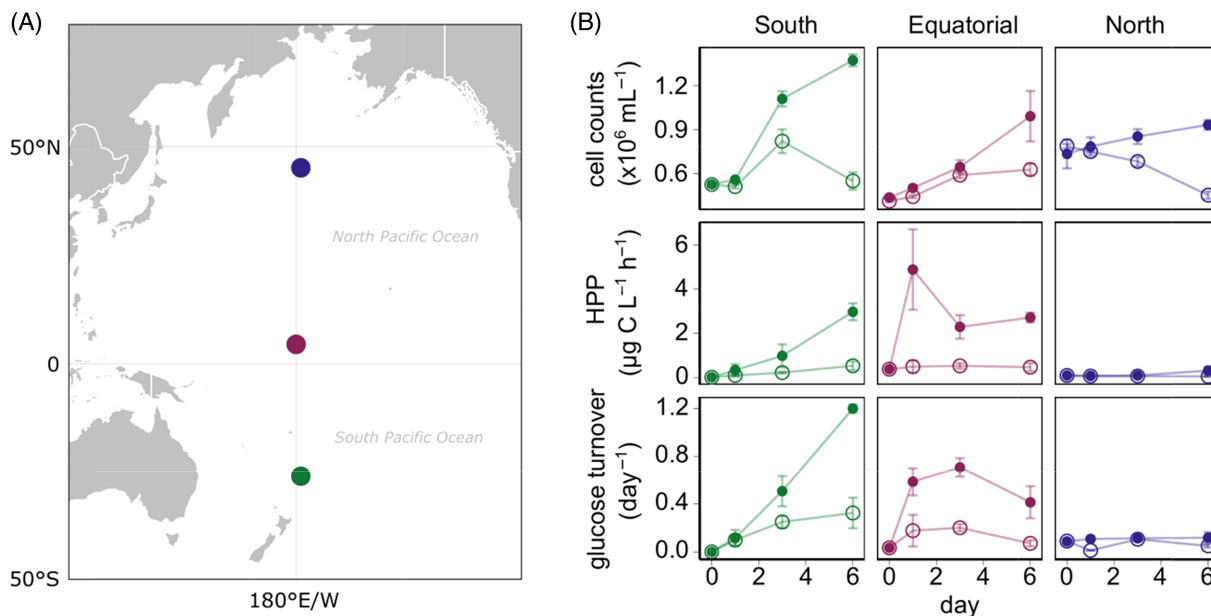


**FIGURE 1** Sites of seawater sampling for mesocosm experiments (A). Cell counts, heterotrophic prokaryotic production (HPP), and glucose turnover over the 6-day incubation period (B). Open and closed circles indicate control and alginate-amended incubations, respectively. Error bars show the standard deviations from triplicate mesocosms. Note the difference in units and scales.

**TABLE 1** Biogeographic origin, depth, and physicochemical characteristics of seawater samples used for incubation experiments.

	South (SPSG)	Equatorial (PNEC)	North (NPPF)
Latitude ( $^{\circ}\text{N}$ )	-27.0	4.7	45.0
Longitude ( $^{\circ}\text{W}$ )	178.2	179.4	178.8
Depth (m)	20	75	20
Temperature ( $^{\circ}\text{C}$ )	25.2	28.6	5.9
Salinity (PSU)	35.6	34.5	33.3
Phosphate ( $\mu\text{M}$ )	—	0.12	1.3
Chlorophyll a ( $\mu\text{g L}^{-1}$ )	0.3	0.2	0.8
Particulate organic carbon ( $\mu\text{g L}^{-1}$ )	55.4	34.7	98.7
Particulate organic nitrogen ( $\mu\text{g L}^{-1}$ )	8.1	4.1	20.5

Note: Phosphate concentration is below the detection limit ( $0.04 \mu\text{M}$ ) in the South Pacific. Negative latitude indicates south ( $^{\circ}\text{S}$ ).

Abbreviations: NPPF, North Pacific Polar Front; PNEC, Pacific North Equatorial Current; PSU, practical salinity units; SPSG, South Pacific Subtropical Gyre.

highest at d6 in the South Pacific ( $1.198 \pm 0.035 \text{ day}^{-1}$ ), compared with d3 in the Equatorial Pacific ( $0.707 \pm 0.078 \text{ day}^{-1}$ ) (Figure 1). Alginate did not substantially stimulate glucose turnover in the North Pacific, similar to trends observed for HPP.

### Varied community compositional shifts in response to alginate

Bacterial communities in ambient waters were compositionally distinct, and their succession in response to alginate—evident in changing alpha- and beta-diversity—exhibited varying trajectories (Figure 2). Based on principal coordinates analysis (PCoA) of Bray–Curtis dissimilarities, bacterial communities clustered primarily

by site and by treatments within each site (Figure 2A). The separation along the first axis was largely based on temperature: warm South Pacific and Equatorial Pacific waters versus cold North Pacific water. In this ordination, clusters of bacterial communities in control versus alginate incubations ranged from separation (Equatorial Pacific) to overlap (North Pacific), indicating variations in the extent of alginate-induced community turnover across sites. These groupings were consistent for both DNA- and RNA-based sequences (Figure S1).

Partitioning beta-diversity (Figure 2B) and alpha-diversity (Figure 2C) by site highlighted finer-resolution differences in community dynamics. Site-specific PCoA for the South and Equatorial Pacific better resolved bacterial community differences in control versus alginate incubations (Figure 2B). In the

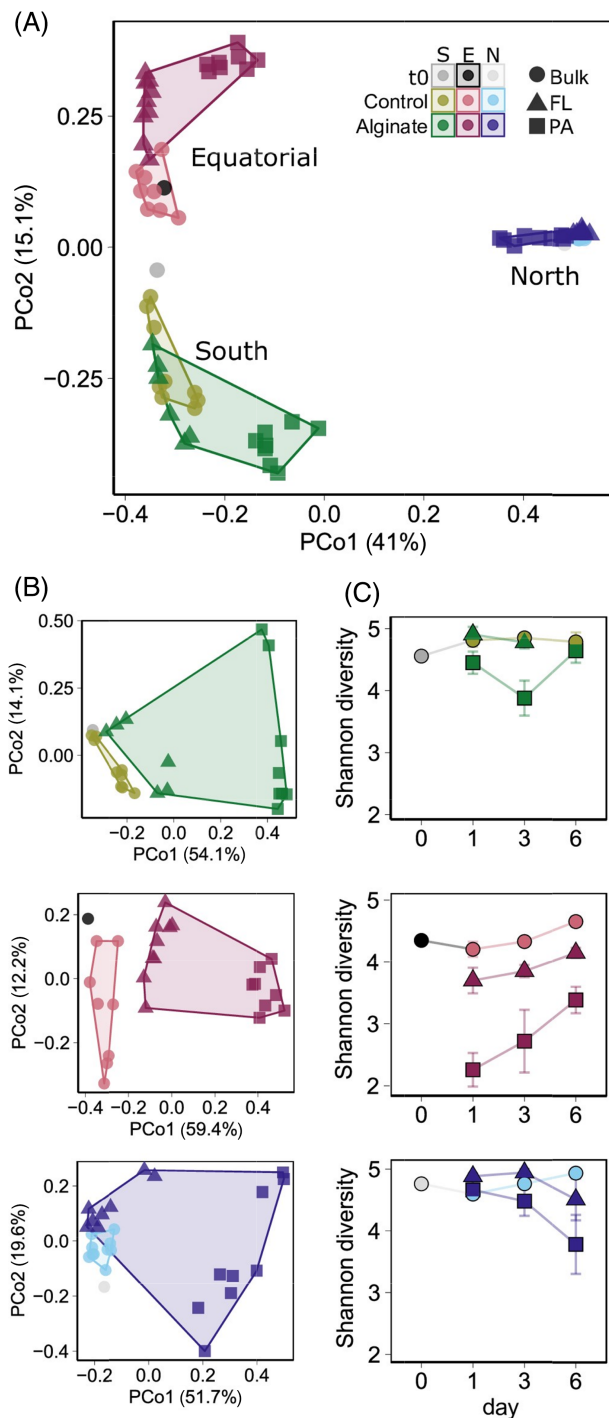


**FIGURE 2** Principal Coordinates Analysis of bacterial community composition using Bray–Curtis dissimilarities at all (A) and individual (B) sites. Mean and standard deviation of Shannon indexed alpha-diversity of triplicate bacterial communities per site (C). All figures share a common legend (top insert in panel A). FL, free-living; PA, particle-associated. No FL data is available in the South Pacific at d6.

North Pacific, bacterial communities in the control moderately overlapped with those in the alginate-FL fraction. The close proximity of FL communities with alginate and the control, as well as the strong

separation of alginate-PA communities, was consistent across the three sites.

Alpha-diversity remained comparable in controls in the South and Equatorial Pacific and was slightly lower in controls in the North Pacific. In contrast, alpha diversity in alginate incubations markedly differed between sites, especially among the PA communities. PA alpha diversity was consistently lowest in the Equatorial Pacific, with minimum values at d1 and an about 150% increase at d3 and d6 (Figure 2C). In the South Pacific, PA alpha diversity decreased from d1 to d3 and increased again at d6. In the North Pacific, PA alpha diversity decreased by about 20% on d6. Alpha diversity for FL communities in the South and North Pacific were similar to those in their respective controls, but not in the Equatorial Pacific.

### Dominant and differentially abundant bacterial taxa

Consistent with PCoA (Figure 2A), the composition of ambient bacterial communities differed between sites. In the South and Equatorial Pacific, *Cyanobiaceae* comprised about 41% of the starting bacterial communities, but only 4% in the North Pacific (Figure 3). This trend was similar for RNA-based sequences but with overall lower values (Figure S2). *Flavobacteriaceae* (19%) was the most abundant family in the North Pacific, followed by SAR11 clade 1 (15%). Several other families—predominantly from classes *Alphaproteobacteria*, *Gammaproteobacteria*, *Bacteroidia*, and *Cyanobacteria*—consistently dominated across sites in the starting community, although their relative proportions differed (Figures 3 and S2–S5).

In the alginate-PA fraction, substantially different proportions of bacterial families across sites (Figure 3) underscore the distinct effect of alginate. In the South Pacific, *Rhodobacteraceae* (15%–29%), *Pseudoalteromonadaceae* (12%–14%), and *Alteromonadaceae* (12%–13%) were most abundant based on DNA sequences (Figure 3), whereas *Cyanobiaceae* was abundant based on RNA sequences (Figure S2). In the Equatorial Pacific, *Alteromonadaceae* dominated alginate-PA communities (52%–79%) whereas *Rhodobacteraceae* constituted low to moderate proportions (3%–12%) with a peak at d6, both with DNA and RNA sequences (Figures 4B and S2). In the North Pacific, *Flavobacteriaceae* (15%–24%) and the SAR116 clade (17%–19%) were the most abundant families throughout the experiment; plus *Pseudoalteromonadaceae* representing 37% of the community at d6 (Figure 3).

For a finer resolution of community dynamics in response to alginate, we identified PA- and FL-ASVs that were enriched with alginate compared with the controls, with more ASVs enriched in the PA compared

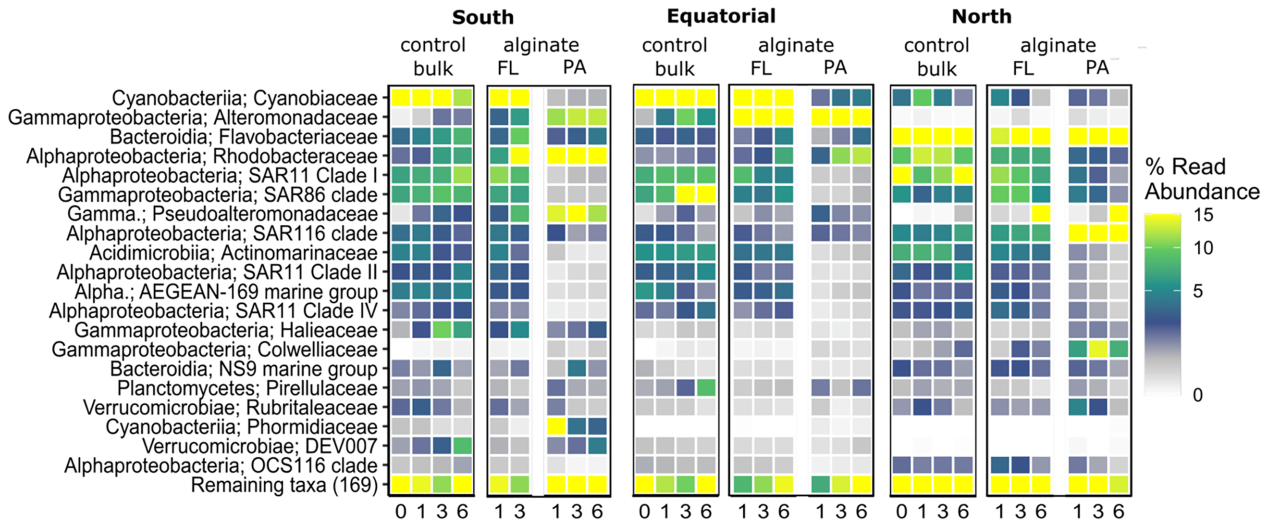


**FIGURE 3** Community composition based on the mean relative proportions (% read abundance) of the top 20 bacterial families. Yellow squares indicate relative proportions of  $\geq 15\%$ . White squares indicate relative proportions below the detection limit. No FL data is available in the South Pacific at d6.

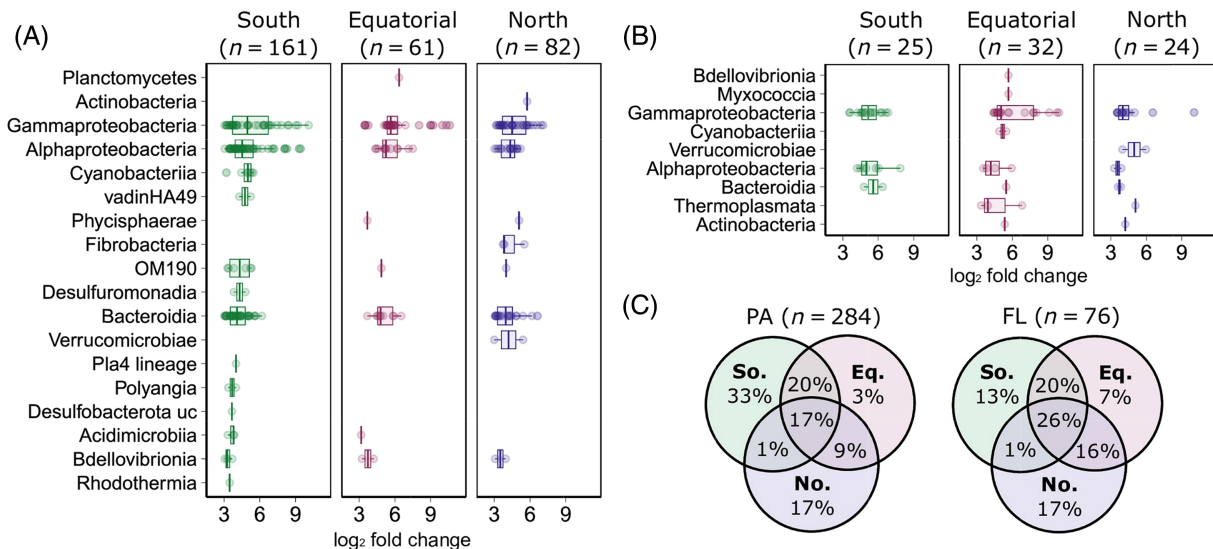


**FIGURE 4** Classes of PA (A) and FL (B) ASVs that are differentially enriched ( $\log_2$  fold change  $\geq 3$ ,  $p < 0.01$ ) in alginate versus control incubations. Counts indicate the number of differentially abundant ASVs identified per site. For visual clarity, one ASV was excluded from (A) and (B) because the  $\log_2$ -fold change was  $>20$ ; these ASVs are still included in the  $n$  counts and in (C). Venn diagrams show the relative proportions of unique differentially abundant ASVs (PA,  $N = 308$ ; FL,  $N = 57$ ) found only at one site, or shared between two or all three sites (C).

with the FL fraction (Figure 4A,B). Altogether, these taxa represent 18 and 9 bacterial classes—corresponding to 63 and 26 families—in the alginate PA and FL fractions, respectively. Most of the differentially abundant taxa belong to *Gammaproteobacteria* (PA = 102, FL = 51), *Alphaproteobacteria* (PA = 81, FL = 13), and *Bacteroidia* (PA = 69, FL = 5). Families *Pseudoalteromonadaceae*, *Alteromonadaceae*, *Rhodobacteraceae*, and *Flavobacteriaceae* were highly abundant in both the PA and FL fractions; *Colwelliaceae* and *Vibrionaceae* were also abundant in the PA and FL fractions, respectively. In total, these ASVs represented

284 unique taxa in the PA and 76 in the FL fraction (Figure 4C), of which 20% were detectable at all sites or two sites. The South Pacific contained the greatest proportion of unique taxa in the PA fraction (37%), compared with almost no unique taxa in the Equatorial Pacific (3%). Only 1% of differentially abundant ASVs were shared between the South and North Pacific. Differentially abundant ASVs represented varying proportions of the total bacterial community: 62%–71% in the South Pacific, 67%–78% in the Equatorial Pacific, and 24%–58% in the North Pacific (PA-ASVs), compared with 6%–14% in the South Pacific, 6%–9% in the

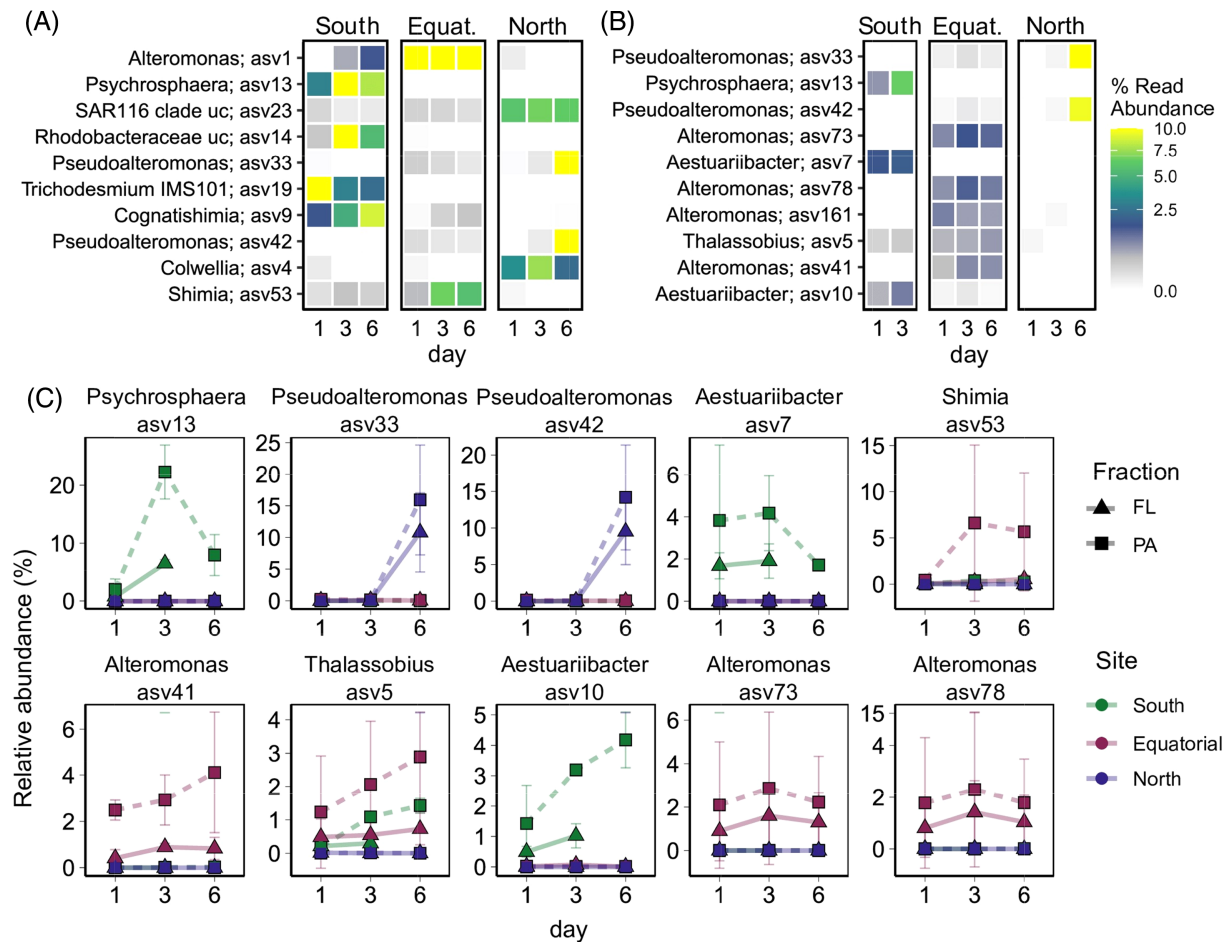


**FIGURE 5** Mean relative proportions of the top 10 differentially abundant bacterial ASVs and associated genera in PA (A) and FL (B) fractions, as well as the top 10 differentially abundant bacterial ASVs shared between PA and FL (C). Yellow squares indicate relative proportions of  $\geq 10\%$ . White squares indicate relative ASV proportions below the detection limit. No FL data is available in the South Pacific at d6.

Equatorial Pacific, and 1%–23% in the North Pacific (FL-ASVs) (Figures S6 and S7; Table S2).

Temporal dynamics greatly varied for PA- and FL-enriched taxa (Figure 5A,B), as well as for taxa shared between PA and FL (Figure 5C). ASVs typically dominated—and therefore were highly differentially abundant—only at one site. For example, in the PA fraction, an *Alteromonas* ASV (asv1) constituted up to 60% in the Equatorial Pacific compared with  $<2\%$  at other sites (Figure 5A). Furthermore, four ASVs—identified as *Psychrosphaera* (asv4), uncultured *Rhodobacteraceae* (asv14), *Trichodesmium* (asv19), and *Cognatishimia* (asv9)—dominated only in the South Pacific, but each at different time points. Similarly, FL-enriched taxa usually dominated only at one site (Figure 5B). Differentially abundant taxa shared between PA and FL showed varying trajectories (Figure 5C). For example, in the North Pacific, the relative proportions of *Pseudoalteromonas* asv33 and asv42 remained close to 0%, until increasing to  $\sim 10\%$  to 16% in the PA and FL fractions at d6. Other taxa showed similar trends across size fractions, such as

*Thalassobius* (asv5), *Alteromonas* (asv73), and *Alteromonas* (asv78), indicating that alginate responses may be similar across size fractions. Different temporal trends between the PA and FL size fractions were uncommon, only seen for *Shimia* asv53.

### Site-dependent shifts in enzymatic activities in response to alginate

To investigate the functional consequences of community responses to alginate, we compared the enzymatic capabilities in control and alginate incubations at the end of the experiment. Enzyme activity from the ambient waters has been previously published (Balmonte et al., 2021), but to provide context here, we describe the most relevant features. Peptidase and glucosidase activities, as well as polysaccharide hydrolase activities, strongly differed across sites. All peptidase and glucosidase activities were measurable in the Equatorial Pacific, compared with the most limited range in the North Pacific (Balmonte et al., 2021). The range of



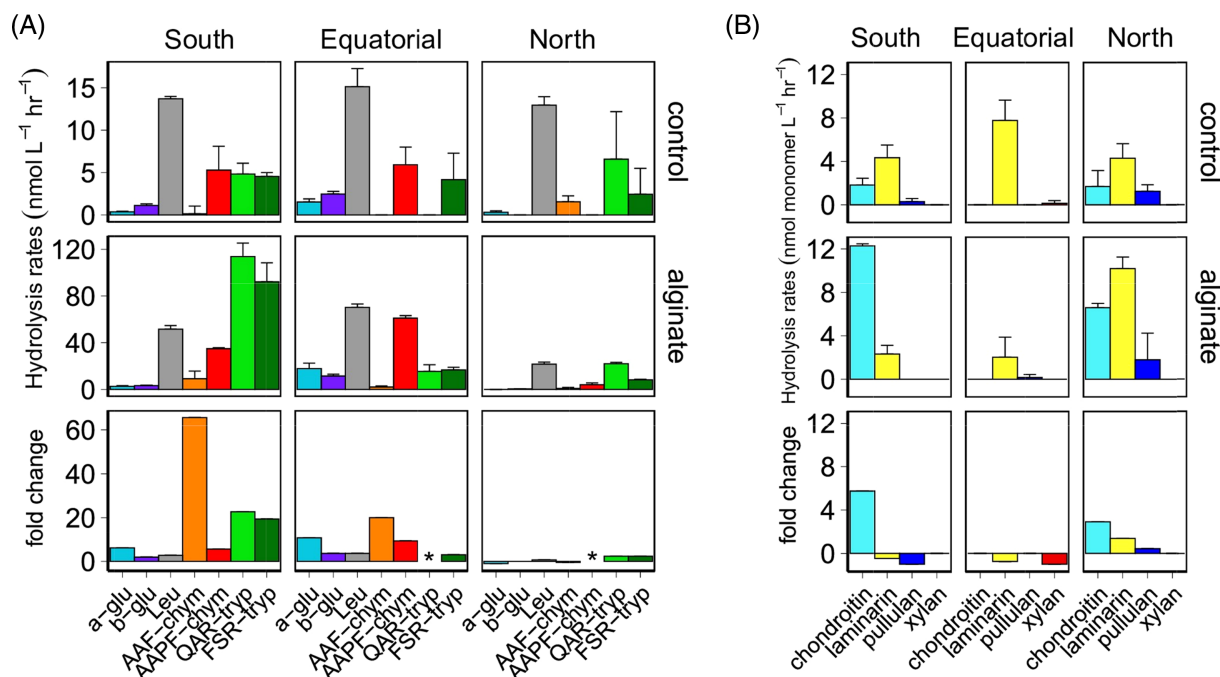


**FIGURE 6** Enzymatic activity rates after 0 and 6 days in control and alginate-amended incubations measured using MUF- and MCA-labelled peptide and glucose substrates (A) and FLA-labelled polysaccharide substrates (B). Note the differences in y-axis scales (A). chym, chymotrypsin; glu, glucosidase; Leu, leucine aminopeptidase; tryp, trypsin. Note asterisks in (A), indicating that fold-changes cannot be calculated, since the corresponding values in the controls were zero.

polysaccharide hydrolase activities was broadest in the South Pacific, and most limited in the Equatorial Pacific. Leucine aminopeptidase and laminarinase activities consistently showed the highest enzymatic rates across stations (Balmonte et al., 2021).

In alginate incubations, enzymatic activities by d6 changed to varying degrees, both across sites and substrates. Although absolute rates were up to an order of magnitude greater with alginate compared with the control, the relative proportions of peptidase and glucosidase activities changed most prominently in the South Pacific (Figure 6A). These shifts were characterized by substantially higher proportions of trypsin activities (e.g., QAR-tryp and FSR-tryp) relative to the other peptidases and glucosidases, and about 20-fold or greater increase in trypsin activities with alginate compared with the control. AAF-chymotrypsin activities showed the strongest response to alginate, with a >60-fold increase compared with the control; this difference was also the highest measured across all enzyme activities and sites (Figure 6A). In the Equatorial Pacific, peptidase and glucosidase activities changed only moderately in response to alginate. AAF-chymotrypsin, AAPF-chymotrypsin, and  $\alpha$ -glucosidase activities increased about 10- to 20-fold with alginate, whereas other peptidase and glucosidase increased about 2- to 3-fold. Enzyme activity changes were more subdued in the North Pacific, with about 2-fold increasing activity by the two trypsins compared with the control. Notably,

the relative proportions of leucine aminopeptidase with alginate decreased across all sites, suggesting increased relative importance of other community-wide peptidase activities.

Shifts in polysaccharide hydrolase activities with alginate were subtle and variable across sites (Figure 6B). Chondroitinase activities increased in the South (6-fold) and North Pacific (3-fold) at d6, but were not measurable in the Equatorial Pacific. Laminarinase activities decreased by about 50% and 75% in the South and Equatorial Pacific, respectively, but nearly doubled in the North Pacific. Minor changes in polysaccharide hydrolase activities in response to alginate strongly contrast with the substantial changes in peptidase activities, especially the endopeptidases (trypsin and chymotrypsin). Hence, alginate-induced community succession might predominantly coincide with changes in peptidase activities as well as in polysaccharide hydrolase activities not measured here.

## DISCUSSION

The influence of alginate availability on microbial dynamics has been widely investigated in coastal systems (Enke et al., 2019; Jain et al., 2020; Mitulla et al., 2016; Thomas et al., 2021), but equivalent studies in open oceans are sparse (Wietz et al., 2015). Our study illustrates ecological and functional changes



upon an alginate pulse in oligotrophic ocean systems, in which nutrient and organic matter concentrations for heterotrophic microorganisms are limited. In open ocean systems, alginate may originate from pelagic taxa such as *Sargassum* or laterally-advected coastal macroalgae (Davis et al., 2021; Rosado-Espinosa et al., 2020; Yip et al., 2020). Our study also provides insights into the broader consequences of resource availability (in this case, a polysaccharide) for microbial compositional and functional succession in marine systems.

The addition of about 0.02 g alginate per litre of seawater—a considerable pulse of carbon relative to ambient conditions—stimulated distinct compositional, metabolic, and enzymatic patterns of microbial communities in subtropical, tropical, and cold Pacific waters. Community succession and its functional consequences were most pronounced in the South Pacific, followed by the Equatorial Pacific and the North Pacific. The rate of community turnover is largely related to different temperatures between sites: rapid in the warm subtropical and equatorial waters, but slow and gradual in the cold waters of the polar front. Distinct alginate-induced responses in the South and Equatorial Pacific—with similar temperatures in surface waters (Table 1) and many shared taxa (Figures 3 and 4C)—may be better explained by other physicochemical and biogeochemical characteristics as well as microbial interactions.

If alginate-induced succession solely relied on starting physicochemical conditions, the strongest and most immediate response would be expected in the Equatorial Pacific. This site featured the lowest POC and PON concentrations and highest water temperature; hence, alginate would alleviate resource scarcity, with microbial response times likely expedited by the warm temperatures. However, the most visible shifts in enzymatic profiles—alongside reduced alpha diversity and an order of magnitude more differentially abundant PA taxa—were observed in the South Pacific. Since this station is within the ultraoligotrophic subtropical gyre, the availability of alginate may have fulfilled scarce resources not measured by our biogeochemical analyses. Microbial communities in the South Pacific may additionally be geared to rapidly exploit resource pulses—an advantageous trait among organisms experiencing resource scarcity. Thus, how communities respond to alginate availability seems to ultimately depend both on starting physicochemical conditions and the ambient microbial community.

Detection of identical ASVs across sites and size fractions, but with different temporal dynamics, underscores the context-dependence of alginate responses (Figure 5). A notable example is *Alteromonas* asv1 (Figure 5A), affiliated with a genus harbouring characterized alginate degraders (Neumann et al., 2015; Thomas et al., 2021). The asv1 amplicon (427 nucleotides) has

100% identity with a 16S rRNA gene fragment of *A. macleodii* BGP6, BGP9, and BGP14, alginolytic strains isolated from the mesocosms analysed here (Koch et al., 2020). Although this indicates that *Alteromonas* asv1 can utilize alginate, its relative proportion in the South and North Pacific remained low—in contrast to its dominance in the PA-alginate fraction in the Equatorial Pacific (Figure 5A). In the South Pacific, abundant ASVs belonged to *Psychrosphaera* from family *Pseudoalteromonadaceae* (Lee et al., 2014; Park et al., 2011), as well as *Cognatishimia* (Park et al., 2010; Wirth & Whitman, 2018) and an uncultured *Rhodobacteraceae*, both from family *Rhodobacteraceae*. While specific members within these families can incorporate alginate (Thomas et al., 2021) or utilize its constituent oligomers (Volter et al., 2021), little is known about the potential of *Psychrosphaera* and *Cognatishimia* for alginate degradation. However, specific members of *Pseudoalteromonadaceae* are known to transcribe alginate lyases in marine systems (Cha et al., 2023). Furthermore, these taxa only dominated in the South Pacific, despite being detected in the Equatorial (up to ca. 1%) and North Pacific (<1%). Missing responses to alginate outside of the South Pacific may not necessarily relate to their low relative proportions, since other taxa (such as *Pseudoalteromonas* asv15 and asv20) became dominant despite initially low relative abundances (Figure 5B). Comparable to our observations in the North Pacific, *Pseudoalteromonas* and *Colwellia* bloomed in the coastal Arctic waters of Svalbard (Jain et al., 2020), indicating consistent responses of some psychrotolerant taxa in cold northerly waters. Similar blooms within *Pseudoalteromonadaceae* and *Colwelliaceae* have been observed in response to other organic matter (Balmonte et al., 2019; Brown et al., 2022). Hence, the response of taxa to alginate may be balanced by competition with other taxa able to exploit this resource; in other words, the surrounding biotic and abiotic environments are just as important as an organism's capabilities.

The greater relative increase of PA compared with FL taxa across all sites in response to alginate may in part be due to their chemotactic abilities (Lambert et al., 2019; Smriga et al., 2016), fast growth rates (Leu et al., 2022), and metabolic flexibility (Balmonte et al., 2021; Boeuf et al., 2019; Zhao et al., 2020). Recent findings showed that alginate particles harbour more taxa encoding alginate lyases than the surrounding water (Bunse et al., 2021). Hence, PA taxa probably initiate the alginate degradation cascade and exploit the substrate before others can access released oligo- and monomers. Enrichment of comparatively fewer FL taxa may partially relate to dual lifestyles with nearly equal prevalence in PA and FL fractions; *Pseudoalteromonas* asv15 and asv20 are notable examples (Figure 5). Alginate mono- and oligomers, as well as metabolic byproducts of the initial responders, may additionally fuel taxa that cannot produce alginate



degradative enzymes—a likely case among FL taxa (Bunse et al., 2021; Enke et al., 2019). Thus, alginate—initially accessible only to a limited range of taxa—probably became a resource for the entire community. An additional explanation for the greater enrichment of PA taxa may relate to the gelling properties of alginate (Abka-Khajouei et al., 2022). In seawater, alginate coagulates and forms a particle matrix that might function as a colonization scaffold, to which microbes attach—or become embedded within—independent of alginolytic capacities. For example, in the South Pacific alginate-PA fraction, the high prevalence of *Trichodesmium* (family *Phormidiaceae*; Figure 3)—a colony-forming cyanobacterium not linked to alginate degradation—may have been the combined result of passive association with the alginate matrix and growth.

A caveat to the analysis of differentially abundant ASVs is that their detection may be biased by experimental limitations (see Section 2.6). In our setup, the signal from the alginate response is mixed with the signal simply due to size fraction (PA vs. FL). Nevertheless, most differentially enriched taxa in alginate incubations, both in PA and FL fractions, are closely related to known alginate degraders, supporting the presence of specific bacterial responses to alginate.

As alginate-induced succession proceeded, enzymatic functions were stimulated to varying degrees among the ambient microbiomes. Increased chymotrypsin and trypsin activities, both in terms of absolute rates and relative proportions, underscore the impact of alginate availability on processes beyond its utilization. These enzymes specifically cleave phenylalanine and arginine moieties, but their significance within the context of alginate in marine environments is unknown. Findings that chymotrypsin and trypsin may be preferentially produced by PA taxa (Lloyd et al., 2022)—particularly at locations where this present study was conducted (Balmonte et al., 2021)—suggest a role in the degradation of particulate matter. The stimulation of chondroitin and laminarin hydrolysis, particularly in the North Pacific, indicates that the addition of one polysaccharide type induces the hydrolysis of others by stimulating microbial generalists, including those associated with particles. Overall, the functional consequences of alginate availability are likely wide-ranging; with specific effects related to alginolytic capacities as well as indirect effects via cross-feeding of metabolic byproducts. Such effects may be long-lasting since most of the enzymatic activities measured in this study increased at d6. Longer-term changes in enzymatic profiles (up to 69 days) following a pulse of high molecular weight organic matter (Balmonte et al., 2019; Brown et al., 2022) substantiate this speculation.

Overall, our study demonstrates that alginate availability drives varying ecological and biogeochemical changes across biogeographical provinces in the

Pacific Ocean. While the speed of succession is partly related to temperature, different dynamics of taxa and their enzymatic activities even in physicochemically similar waters (Table 1) underscore the context-dependence of these trajectories. Differences in microbial dynamics likely determine the outcome of resource pulses in contrasting biogeographic provinces harbouring specific microbiomes. The demonstrated geographic variability in compositional and functional responses suggests that the same polysaccharide pulse may diversify the ambient organic matter pool across latitudes, partly promoted by metabolic byproducts of microbes that differentially respond during succession.

## AUTHOR CONTRIBUTIONS

**John Paul Balmonte:** Conceptualization (supporting); data curation (equal); formal analysis (equal); investigation (equal); methodology (equal); resources (equal); visualization (lead); writing – original draft (lead); writing – review and editing (lead). **Helge-Ansgar Giebel:** Conceptualization (equal); data curation (equal); investigation (equal); methodology (equal); resources (equal); supervision (equal); writing – original draft (supporting); writing – review and editing (supporting). **Carol Arnosti:** Conceptualization (supporting); data curation (supporting); investigation (equal); methodology (equal); resources (equal); supervision (supporting); writing – original draft (supporting); writing – review and editing (supporting). **Meinhard Simon:** Conceptualization (equal); funding acquisition (lead); methodology (equal); project administration (equal); resources (equal); supervision (equal); writing – original draft (supporting); writing – review and editing (supporting). **Matthias Wietz:** Conceptualization (lead); data curation (equal); formal analysis (equal); investigation (equal); methodology (equal); project administration (equal); resources (equal); supervision (lead); writing – original draft (lead); writing – review and editing (lead).

## ACKNOWLEDGEMENTS

We are grateful to the captain, crew, and scientific party of R/V *Sonne* for their tireless work and support during the SO248 BacGeoPac cruise. In particular, we thank Laura Wolter, Marco Dogs, Mathias Wolterink, Birgit Kürzel, Gerrit Wienhausen, Felix Milke, Sara Billerbeck, Nils Bergen, Insa Bakenhus, Mara Heinrichs, and Jürgen Tomasch for help with sample collection and processing. We thank Thomas Badewien and Holger Winkler for the CTD operation. Mads Albertsen and colleagues at DNASense are acknowledged for amplicon sequencing. Finally, we thank Sherif Ghobrial and Karylle Abella for their assistance with sample processing. The SO248 cruise was funded by the German Federal Ministry of Education and Research (BMBF) within the BacGeoPac project (03G0248A). JPB and CA were supported by NSF (OCE-1332881 and OCE-1736772



to CA). JPB was also supported by a UNC Global Partnership Award. HAG and MS were supported by Deutsche Forschungsgemeinschaft (DFG) within the Collaborative Research Center Roseobacter (TRR51). MW was supported by DFG grant WI3888/1-2.

## CONFLICTS OF INTEREST STATEMENT

The authors have no conflicts of interest to declare.

## DATA AVAILABILITY STATEMENT


Physicochemical data are available at Pangaea: <https://doi.org/10.1594/PANGAEA.864673> (Badewien et al., 2016). Microbial parameters, including cell counts, heterotrophic prokaryotic production, and glucose turnover, are available at <https://doi.pangaea.de/10.1594/PANGAEA.918500> (Giebel et al., 2020) and as Supporting Information (Table S1). 16S rRNA amplicon sequences have been deposited in the European Nucleotide Archive under accession number PRJEB61534: <https://www.ebi.ac.uk/ena/browser/view/PRJEB61534>. Metadata and accession numbers of fastq files are available in Table S2. Enzyme activity data are available in Table S3. The complete analysis workflow is available at <https://github.com/matthiaswietz/pacific-alginate>.

## ORCID

John Paul Balmonde  <https://orcid.org/0000-0001-5571-4893>

Helge-Ansgar Giebel  <https://orcid.org/0000-0002-9452-0810>

Carol Arnosti  <https://orcid.org/0000-0002-6074-5341>

Meinhard Simon  <https://orcid.org/0000-0002-6151-6989>

Matthias Wietz  <https://orcid.org/0000-0002-9786-3026>

## REFERENCES

- Abka-Khajouei, R., Tounsi, L., Shahabi, N., Patel, A.K., Abdelkafi, S. & Michaud, P. (2022) Structures, properties, and applications of alginates. *Marine Drugs*, 20(6), 364. Available from: <https://doi.org/10.3390/md20060364>
- Amon, R.M.W. & Benner, R. (1996) Bacterial utilization of different size classes of dissolved organic matter. *Limnology and Oceanography*, 41(1), 41–51. Available from: <https://doi.org/10.4319/lo.1996.41.1.0041>
- Arnosti, C. (2003) Fluorescent derivatization of polysaccharides and carbohydrate-containing biopolymers for measurement of enzyme activities in complex media. *Journal of Chromatography B: Analytical Technologies in the Biomedical and Life Sciences*, 793(1), 181–191. Available from: [https://doi.org/10.1016/S1570-0232\(03\)00375-1](https://doi.org/10.1016/S1570-0232(03)00375-1)
- Arnosti, C. (2011) Microbial extracellular enzymes and the marine carbon cycle. *Annual Review of Marine Science*, 3, 401–425. Available from: <https://doi.org/10.1146/annurev-marine-120709-142731>
- Arnosti, C., Steen, A.D., Ziervogel, K., Ghobrial S., Jeffrey W.H. (2011) Latitudinal gradients in degradation of marine dissolved organic carbon. *PLoS One*, 6, e28900. <https://doi.org/10.1371/journal.pone.0028900>
- Arnosti, C., Wietz, M., Brinkhoff, T., Hehemann, J.-H., Probandt, D., Zeugner, L. et al. (2021) The biogeochemistry of marine polysaccharides: sources, inventories, and bacterial drivers of the carbohydrate. *Cycle*, 13, 81–108. Available from: <https://doi.org/10.1146/annurev-marine-032020-012810>
- Badewien, T.H., Winkler, H., Arndt, K.L. & Simon, M. (2016) *Physical oceanography during SONNE cruise SO248 (BacGeoPac)*. PANGAEA: Institute for Chemistry and Biology of the Marine Environment, Carl-von-Ossietzky University of Oldenburg. <https://doi.org/10.1594/PANGAEA.864673>
- Balmonde, J.P., Buckley, A., Hoarfrost, A., Ghobrial, S., Ziervogel, K., Teske, A. et al. (2019) Community structural differences shape microbial responses to high molecular weight organic matter. *Environmental Microbiology*, 21(2), 557–571. Available from: <https://doi.org/10.1111/1462-2920.14485>
- Balmonde, J.P., Simon, M., Giebel, H.A. & Arnosti, C. (2021) A sea change in microbial enzymes: heterogeneous latitudinal and depth-related gradients in bulk water and particle-associated enzymatic activities from 30° S to 59° N in the Pacific Ocean. *Limnology and Oceanography*, 66(9), 3489–3507. Available from: <https://doi.org/10.1002/lno.11894>
- Balmonde, J.P., Teske, A. & Arnosti, C. (2018) Structure and function of high Arctic pelagic, particle-associated and benthic bacterial communities. *Environmental Microbiology*, 20(8), 2941–2954. Available from: <https://doi.org/10.1111/1462-2920.14304>
- Boeuf, D., Edwards, B.R., Eppley, J.M., Hu, S.K., Poff, K.E., Romano, A.E. et al. (2019) Biological composition and microbial dynamics of sinking particulate organic matter at abyssal depths in the oligotrophic open ocean. *Proceedings of the National Academy of Sciences of the United States of America*, 116(24), 11824–11832. Available from: <https://doi.org/10.1073/pnas.1903080116>
- Brown, S.A., Balmonde, J.P., Hoarfrost, A., Ghobrial, S. & Arnosti, C. (2022) Depth-related patterns in microbial community responses to complex organic matter in the western North Atlantic Ocean. *Biogeosciences*, 19(24), 5617–5631. Available from: <https://doi.org/10.5194/bg-19-5617-2022>
- Bunse, C., Koch, H., Breider, S., Simon, M. & Wietz, M. (2021) Sweet spheres: succession and CAzyme expression of marine bacterial communities colonizing a mix of alginate and pectin particles. *Environmental Microbiology*, 23(6), 3130–3148. Available from: <https://doi.org/10.1111/1462-2920.15536>
- Callahan, B.J., McMurdie, P.J., Rosen, M.J., Han, A.W., Johnson, A.J.A. & Holmes, S.P. (2016) DADA2: high-resolution sample inference from Illumina amplicon data. *Nature Methods*, 13(7), 581–583. Available from: <https://doi.org/10.1038/nmeth.3869>
- Cha, Q.Q., Liu, S.S., Dang, Y.R., Ren, X.B., Xu, F., Li, P.Y. et al. (2023) Ecological function and interaction of different bacterial groups during alginate processing in coastal seawater community. *Environment International*, 182, 108325.
- Cheng, D., Jiang, C., Xu, J., Liu, Z. & Mao, X. (2020) Characteristics and applications of alginate lyases: a review. *International Journal of Biological Macromolecules*, 164, 1304–1320. Available from: <https://doi.org/10.1016/j.ijbiomac.2020.07.199>
- Davis, D., Simister, R., Campbell, S., Marston, M., Rose, B., McQueen-Mason, S.J. et al. (2021) Biomass composition of the golden tide pelagic seaweeds *Sargassum fluitans* and *S. natans* (morphotypes I and VIII) to inform valorisation pathways. *Science of the Total Environment*, 762, 143134. Available from: <https://doi.org/10.1016/j.scitotenv.2020.143134>
- Draget, K.I., Smidsrød, O. & Skjåk-Bræk, G. (2005) Alginates from algae. *Biopolymers*. Available from: <https://doi.org/10.1002/3527600035.bpol6008>
- Enke, T.N., Datta, M.S., Schwartzman, J., Cermak, N., Schmitz, D., Barrere, J. et al. (2019) Modular assembly of polysaccharide-degrading marine microbial communities. *Current Biology*, 29(9),



- 1528–1535. Available from: <https://doi.org/10.1016/j.cub.2019.03.047>
- Giebel, H.-A., Aldag, P., Arndt, K.L., Arnosti, C., Badewien, T.H. & Bakenhus, I. (2020) *Hydrography, biogeochemistry, microbial population, growth and substrate dynamics between subarctic and subantarctic waters in the Pacific Ocean during the cruises SO248 and SO254 with RV Sonne*. Bremerhaven: PANGAEA. Available from: <https://doi.org/10.1594/PANGAEA.918500>
- Giebel, H.A., Arnosti, C., Badewien, T.H., Bakenhus, I., Balmonte, J.P., Billerbeck, S. et al. (2021) Microbial growth and organic matter cycling in the Pacific Ocean along a latitudinal transect between subarctic and subantarctic waters. *Frontiers in Marine Science*, 8, 1–19. Available from: <https://doi.org/10.3389/fmars.2021.764383>
- Hoarfrost, A., Balmonte, J.P., Ghobrial, S., Ziervogel, K., Bane, J., Gawarkiewicz, G. et al. (2019) Gulf stream ring water intrusion on the mid-Atlantic bight continental shelf break affects microbially driven carbon cycling. *Frontiers in Marine Science*, 6, 1–13. Available from: <https://doi.org/10.3389/fmars.2019.00394>
- Hoppe, H.G. (1983) Significance of exoenzymatic activities in the ecology of brackish water: measurements by means of methylumbelliferyl-substrates. *Marine Ecology-Progress Series Impact*, 11, 299–308. <https://doi.org/10.3354/meps011299>
- Jain, A., Krishnan, K.P., Begum, N., Singh, A., Thomas, F.A. & Gopinath, A. (2020) Response of bacterial communities from Kongsfjorden (Svalbard, Arctic Ocean) to macroalgal polysaccharide amendments. *Marine Environmental Research*, 155, 104874. Available from: <https://doi.org/10.1016/j.marenvres.2020.104874>
- Klindworth, A., Pruesse, E., Schweer, T., Peplies, J., Quast, C., Horn, M. et al. (2013) Evaluation of general 16S ribosomal RNA gene PCR primers for classical and next-generation sequencing-based diversity studies. *Nucleic Acids Research*, 41(1), e1. Available from: <https://doi.org/10.1093/nar/gks080>
- Koch, H., Dürwald, A., Schweder, T., Noriega-Ortega, B., Vidal-Melgosa, S., Hehemann, J.H. et al. (2019) Biphasic cellular adaptations and ecological implications of *Alteromonas macleodii* degrading a mixture of algal polysaccharides. *ISME Journal*, 13(1), 92–103. Available from: <https://doi.org/10.1038/s41396-018-0252-4>
- Koch, H., Germscheid, N., Freese, H.M., Noriega-Ortega, B., Lücking, D., Berger, M. et al. (2020) Genomic, metabolic and phenotypic variability shapes ecological differentiation and intra-species interactions of *Alteromonas macleodii*. *Scientific Reports*, 10(1), 809. Available from: <https://doi.org/10.1038/s41598-020-57526-5>
- Lambert, B.S., Fernandez, V.I. & Stocker, R. (2019) Motility drives bacterial encounter with particles responsible for carbon export throughout the ocean. *Limnology and Oceanography Letters*, 4(5), 113–118. Available from: <https://doi.org/10.1002/lo.10113>
- Lee, J.H., Baik, K.S., Kim, D. & Seong, C.N. (2014) *Psychrosphaera aestuarii* sp. nov. and *Psychrosphaera haliotis* sp. nov., isolated from the marine environment, and emended description of the genus *Psychrosphaera*. *International Journal of Systematic and Evolutionary Microbiology*, 64, 1952–1957. Available from: <https://doi.org/10.1099/ijs.0.061564-0>
- Leu, A.O., Eppley, J.M., Burger, A. & DeLong, E.F. (2022) Diverse genomic traits differentiate sinking-particle-associated versus free-living microbes throughout the oligotrophic open ocean water column. *MBio*, 13(4), e0156922. Available from: <https://doi.org/10.1128/mbio.01569-22>
- Lloyd, C.C., Brown, S., Balmonte, J.P., Hoarfrost, A., Ghobrial, S. & Arnosti, C. (2022) Particles act as ‘specialty centers’ with expanded enzymatic function throughout the water column in the western North Atlantic. *Frontiers in Microbiology*, 13, 1–16. Available from: <https://doi.org/10.3389/fmicb.2022.882333>
- Love, M.I., Huber, W. & Anders, S. (2014) Moderated estimation of fold change and dispersion for RNA-seq data with DESeq2. *Genome Biology*, 15(12), 550. Available from: <https://doi.org/10.1186/s13059-014-0550-8>
- Milke, F., Wagner-Dobler, I., Wienhausen, G. & Simon, M. (2022) Selection, drift and community interactions shape microbial biogeographic patterns in the Pacific Ocean. *The ISME Journal*, 16, 2653–2665. Available from: <https://doi.org/10.1038/s41396-022-01318-4>
- Mitulla, M., Dinasquet, J., Guillemette, R., Simon, M., Azam, F. & Wietz, M. (2016) Response of bacterial communities from California coastal waters to alginate particles and an alginolytic *Alteromonas macleodii* strain. *Environmental Microbiology*, 18(12), 4369–4377. Available from: <https://doi.org/10.1111/1462-2920.13314>
- Neumann, A.M., Balmonte, J.P., Berger, M., Giebel, H.A., Arnosti, C., Voget, S. et al. (2015) Different utilization of alginate and other algal polysaccharides by marine *Alteromonas macleodii* ecotypes. *Environmental Microbiology*, 17(10), 3857–3868. Available from: <https://doi.org/10.1111/1462-2920.12862>
- Park, S., Lee, M.H., Lee, J.S., Oh, T.K. & Yoon, J.H. (2011) *Thalassobius maritimus* sp. nov., isolated from seawater. *International Journal of Systematic and Evolutionary Microbiology*, 62(1), 8–12. Available from: <https://doi.org/10.1099/ijs.0.029199-0>
- Park, S., Yoshizawa, S., Hamasaki, K., Kogure, K. & Yokota, A. (2010) *Psychrosphaera saromensis* gen. nov., sp. nov., within the family Pseudoalteromonadaceae, isolated from Lake Saroma, Japan. *Journal of General and Applied Microbiology*, 56, 475–480.
- Quast, C., Pruesse, E., Yilmaz, P., Gerken, J., Schweer, T., Yarza, P. et al. (2013) The SILVA ribosomal RNA gene database project: improved data processing and web-based tools. *Nucleic Acids Research*, 41(D1), D590–D596. Available from: <https://doi.org/10.1093/nar/gks1219>
- Rehm, B.H.A. (2009) *Alginates: biology and applications*. Microbiology monographs. Berlin: Springer.
- Reintjes, G., Arnosti, C., Fuchs, B.M. & Amann, R. (2017) An alternative polysaccharide uptake mechanism of marine bacteria. *ISME Journal*, 11(7), 1640–1650. Available from: <https://doi.org/10.1038/ismej.2017.26>
- Rosado-Espinosa, L.A., Freile-Pelegrin, Y., Hernandez-Nunez, E. & Robledo, D. (2020) A comparative study of Sargassum species from the Yucatan Peninsula coast: morphological and chemical characterisation. *Phycologia*, 59(3), 261–271. Available from: <https://doi.org/10.1080/00318884.2020.1738194>
- Schneider, D., Wemheuer, F., Pfeiffer, B. & Wemheuer, B. (2017) Extraction of total DNA and RNA from marine filter samples and generation of a cDNA as universal template for marker gene studies. *Methods in Molecular BIOLOGY*, 1539, 13–22. Available from: [https://doi.org/10.1007/978-1-4939-6691-2\\_2](https://doi.org/10.1007/978-1-4939-6691-2_2)
- Sichert, A., Corzett, C.H., Schechter, M.S., Unfried, F., Markert, S. et al. (2020) Verrucomicrobia use hundreds of enzymes to digest the algal polysaccharide fucoidan. *Nature Microbiology*, 5, 1026–1039. <https://doi.org/10.1038/s41564-020-0720-2>
- Simon, M. & Azam, F. (1989) Protein content and protein synthesis rates of planktonic marine bacteria. *Marine Ecology Progress Series*, 51, 201–213.
- Simon, M. & Rosenstock, B. (2007) Different coupling of dissolved amino acid, protein, and carbohydrate turnover to heterotrophic picoplankton production in the Southern Ocean in austral summer and fall. *Limnology and Oceanography*, 52(1), 85–95. Available from: <https://doi.org/10.4319/lo.2007.52.1.0085>
- Simon, M., Rosenstock, B. & Zwisler, W. (2004) Coupling of epipelagic and mesopelagic heterotrophic picoplankton production to phytoplankton biomass in the Antarctic polar frontal region. *Limnology and Oceanography*, 49(4 I), 1035–1043. Available from: <https://doi.org/10.4319/lo.2004.49.4.1035>
- Smriga, S., Fernandez, V.I., Mitchell, J.G. & Stocker, R. (2016) Chemotaxis toward phytoplankton drives organic matter partitioning among marine bacteria. *Proceedings of the National Academy*



- of *Sciences of the United States of America*, 113(6), 1576–1581. Available from: <https://doi.org/10.1073/pnas.1512307113>
- Teeling, H., Fuchs, B.M., Becher, D., Klockow, C., Gardebrecht, A., Bennke, C.M. et al. (2012) Substrate-controlled succession of marine bacterioplankton populations induced by a phytoplankton bloom. *Science*, 336, 608–611.
- Thomas, F., Barbeyron, T., Tonon, T., Génicot, S., Czik, M. & Michel, G. (2012) Characterization of the first alginolytic operons in a marine bacterium: from their emergence in marine Flavobacteria to their independent transfers to marine Proteobacteria and human gut Bacteroides. *Environmental Microbiology*, 14(9), 2379–2394. Available from: <https://doi.org/10.1111/j.1462-2920.2012.02751.x>
- Thomas, F., le Duff, N., di Wu, T., Cébron, A., Uroz, S., Riera, P. et al. (2021) Isotopic tracing reveals single-cell assimilation of a macroalgal polysaccharide by a few marine Flavobacteria and Gammaproteobacteria. *ISME Journal*, 15(10), 3062–3075. Available from: <https://doi.org/10.1038/s41396-021-00987-x>
- Traving, S.J., Thygesen, U.H., Riemann, L., Stedmon, C.A. (2015) A model of extracellular enzymes in free-living microbes: which strategy pays off? *Applied and Environmental Microbiology*, 81, 7385–7393. <https://doi.org/10.1128/AEM.02070-15>
- Wietz, M., Wemheuer, B., Simon, H., Giebel, H.A., Seibt, M.A., Daniel, R. et al. (2015) Bacterial community dynamics during polysaccharide degradation at contrasting sites in the southern and Atlantic oceans. *Environmental Microbiology*, 17(10), 3822–3831. Available from: <https://doi.org/10.1111/1462-2920.12842>
- Wirth, J.S. & Whitman, W.B. (2018) Phylogenomic analyses of a clade within the roseobacter group suggest taxonomic reassignments of species of the genera *Aestuaria*, *Citricella*, *Loktanelia*, *Nautella*, *Pelagibaca*, *Ruegeria*, *Thalassobius*, *Thiobacimonas* and *Tropicibacter*, and the proposal of six novel genera. *International Journal of Systematic and Evolutionary Microbiology*, 68(7), 2393–2411. Available from: <https://doi.org/10.1099/ijsem.0.002833>
- Wolter, L.A., Wietz, M., Ziesche, L., Breider, S., Leinberger, J., Poehlein, A. et al. (2021) *Pseudoceanicola algae* sp. nov., isolated from the marine macroalga *Fucus spiralis*, shows genomic and physiological adaptations for an algae-associated lifestyle. *Systematic and Applied Microbiology*, 44(1), 126166. Available from: <https://doi.org/10.1016/j.syapm.2020.126166>
- Yip, Z.T., Quek, R.Z.B. & Huang, D. (2020) Historical biogeography of the widespread macroalga *Sargassum* (Fucales, Phaeophyceae). *Journal of Phycology*, 56(2), 300–309. Available from: <https://doi.org/10.1111/jpy.12945>
- Zhao, Z., Baltar, F. & Herndl, G.J. (2020) Linking extracellular enzymes to phylogeny indicates a predominantly particle-associated lifestyle of deep-sea prokaryotes. *Science Advances*, 6, eaaz4354.

## SUPPORTING INFORMATION

Additional supporting information can be found online in the Supporting Information section at the end of this article.

**How to cite this article:** Balmonte, J.P., Giebel, H.-A., Arnosti, C., Simon, M. & Wietz, M. (2024) Distinct bacterial succession and functional response to alginate in the South, Equatorial, and North Pacific Ocean. *Environmental Microbiology*, 26(3), e16594. Available from: <https://doi.org/10.1111/1462-2920.16594>